We are IntechOpen, the world's leading publisher of Open Access books Built by scientists, for scientists

4,800
Open access books available

122,000
International authors and editors

135M
Downloads

Our authors are among the

154
Countries delivered to

TOP 1%
most cited scientists

12.2%
Contributors from top 500 universities

CLARIVATE ANALYTICS BOOK CITATION INDEX INDEXED

WEB OF SCIENCE™

Selection of our books indexed in the Book Citation Index in Web of Science™ Core Collection (BKCI)

Interested in publishing with us?
Contact book.department@intechopen.com

Numbers displayed above are based on latest data collected.
For more information visit www.intechopen.com

17

Evaluation of Mobility, Diffusion Coefficient and Density of Charge Carriers in Ionic Liquids and Novel Electrolytes Based on a New Model for Dielectric Response

T.M.W.J. Bandara[1,2] and B.-E. Mellander[1]
[1]*Department of Applied Physics, Chalmers University of Technology, Göteborg,*
[2]*Department of Physical Sciences, Rajarata University of Sri Lanka, Mihintale,*
[1]*Sweden*
[2]*Sri Lanka*

1. Introduction

Ionic conductors are key components for many electrochemical applications, mainly in the field of energy conversion, for example, in photo-electrochemical (PEC) solar cells and fuel cells, in energy storage devices like batteries and in other technological applications like electro-chromic devices, super-capacitors, electrochemical sensors [1,2], separation membranes [3], new types of memory and computer architecture as well as in biomedical applications [4,5]. In the last few decades ionic conductors have gained a revolutionary development owing to intense research inspired by their potential use in many electrochemical device applications. However, improved electrolytes are necessary in order to optimize the performance of the device applications. Hence, the need for new electrolytes with improved property regarding conductivity, stability, durability and operating temperature range has called for solutions involving ionic liquids in solid or gel polymer electrolytes.

The enormous number of research articles published in this field proves the broadening of a worldwide research interest on these materials. However, despite the present outstanding development of electrolyte materials, most of the theoretical advancement in this field goes far back, nearly half a century. Hence, to develop theories applicable for these newly developed electrolytes as well as for traditional electrolytes is vitally important for the advancement of the field.

The most important property of an electrolyte is the ionic conductivity, σ_{dc}, and that of an ionic conductor containing many ionic species can be described by,

$$\sigma_{dc} = \sum n_i e |Z_i| \mu_i \tag{1}$$

where n_i is the number of charge carriers per unit volume, μ_i the mobility, Z_i the valance for the ionic species i in the electrolyte and e is the electronic charge. For a system containing one type of cation and one type of anion equation (1) can be modified as,

$$\sigma = n\_e\left|Z^{-}\right|\mu\_ + n_{+}e\left|Z^{+}\right|\mu_{+} \quad (2)$$

where $n_{+}, n\_$ are the number of positive and negative charge carriers per unit volume respectively, e is the electronic charge, $\mu_{+}, \mu\_$ are the mobility of the cation and anion and $Z^{+}, Z,^{-}$ are the valance of the positive and negative charge carriers. The mean mobility (μ) of two ionic species is defined as,

$$\mu = (n\_\mu\_ + n_{+}\mu_{+}) / n \quad (3)$$

where n is the total charge carrier density ($n = n_{+} + n\_$). If we consider the case where the valance of both the cation and the anion are one, then equation (3) can be simplified to,

$$\sigma_{\mathrm{dc}} = ne\mu \quad (4)$$

Hence, in order to obtain a high ionic conductivity the charge carrier density, n, and the mobility, μ, should thus be as high as possible. However, to determine n and μ values is not an easy task although desirable in order to optimize such parameters in electrolytes. On the other hand, the study of n and μ is not only important for the characterization and development of good quality electrolytes for electrochemical device applications but also for other applications, for example it can be employed to quantify the density of viable biological cells in suspensions [6]. A number of approaches have been made to determine ion mobility under an applied electric field, including impedance spectroscopic methods. Transient ionic direct current measurements have also been used to determine the ion mobility [7,8]. This method employs a *dc* voltage until a steady state is reached after which the voltage is reversed and the current is measured as a function of time in order to determine the mobility. Nuclear Magnetic Resonance, NMR, spectroscopy has also been used to obtain this type of information, for instance, NMR has been applied for ionic liquids and polymer electrolytes however there are limitations. For example, the NMR method cannot be employed for all types of ionic species. [9]. However, despite a number of efforts, the mechanisms of ion conduction are still not well understood in many systems [10,11] and in particular there is still some controversy about the values of ion mobility in some solid-state electrolyte systems [11]. Therefore, a reliable and convenient method to determine the mobility and density of charge carriers is required.

Impedance analysis has advantages compared to potentiometric and amperometric electrochemical analysis in that a small perturbation potential is applied across the cell or electrolyte minimizing possible charge carrier concentration changes during the measurements. In impedance analysis, the voltage applied is very small and the time average of the changes, due to the applied sinusoidal potential, is zero. Some committed approaches to determine the mobility and charge carrier concentration based on impedance spectroscopic methods have been reported in the literature [6,11,12]. However none of the methods have been stated to be applicable for liquid electrolytes where simple tests can be used to assess the accuracy. The method used by Schütt *et al* [13] for ion conducting glasses is interesting; in that method the frequency that is selected for the calculations is the one where the real part of the dielectric constant is ten times that of the high frequency plateau ($\varepsilon'_{\mathrm{HF}}$) value. Another recently developed model by Runt *et al* uses the frequency dependence of complex dielectric loss, ε'', and loss tangent, $\tan(\phi)$, data in order to extract both the ion mobility and the mobile ion concentration [11]. This method is based on an analysis of

electrode polarization at low frequency electric fields. However, the values obtained for the mobile charge carrier concentrations are very low, nearly four orders of magnitude lower than that of the total number of ions available in the salt. As a consequence of this the analysis leads to very high mobility values for such solid electrolytes.

This chapter is basically aimed at developing a method to calculate the mobile charge carrier concentration and the mobility using impedance spectroscopic data which should be applicable for a wide range of electrolytes including ionic liquids. This new approach to determine n and μ values is basically based on the studies by Coelho [14], Schütt and Gerdes [15,16] and by Jönsson *et al* [6]. In this work, new equations were derived to determine the charge carrier concentration and the mobility by modeling the space charge relaxation, and the required parameters can be obtained using boundary values of the dielectric function or using curve fitting to the dielectric function. The method is tested with known liquid electrolytes and then applied for various ionic liquids and polymer electrolytes containing an ionic liquid.

2. Theory

2.1 Impedance and impedance analysis

The standard widely used method to determine the bulk ionic conductivity of an electrolyte is complex impedance analysis. The electrical behaviour under an applied electric signal of an electrolyte sandwiched between two blocking electrodes can in the simplest case be described by the equivalent circuit and schematic diagram of a sample cell in Figure 1. When an electrical signal with angular frequency ω is applied to the sample cell negative and positive ions are accumulated at the relevant interfaces of the electrodes as shown in the Figure 1, forming the well known Helmholtz double layer. These two double layers, result in electrode polarization and they behave as two capacitors with capacitance C_e. The geometrical capacitance, C, of the capacitor is formed by the electrolyte and two electrodes (without considering double layer capacitance) and R represents the bulk resistance of the electrolyte. In a real cell a more intricate equivalent circuit is needed to fully describe the electric behaviour but this simple model is sufficient for the moment.

The impedance of a capacitance is purely imaginary and its reactance is given by $1/j\omega C$ where, $j = \sqrt{-1}$. Thus, the total impedance for an electrolyte with blocking electrodes can be represented by,

$$Z^*_{(\omega)} = \frac{R}{1 + j\omega RC} + \frac{2}{j\omega C_e} \tag{5}$$

Therefore, by means of equivalent circuits the real and imaginary parts of the impedance of an electrolyte in blocking electrodes can be represented by,

$$Z' = \frac{R}{1 + \omega^2 R^2 C^2} \tag{6}$$

and

$$Z'' = -\left(\frac{\omega R^2 C}{1 + \omega^2 C^2 R^2} + \frac{2}{\omega C_e} \right) \tag{7}$$

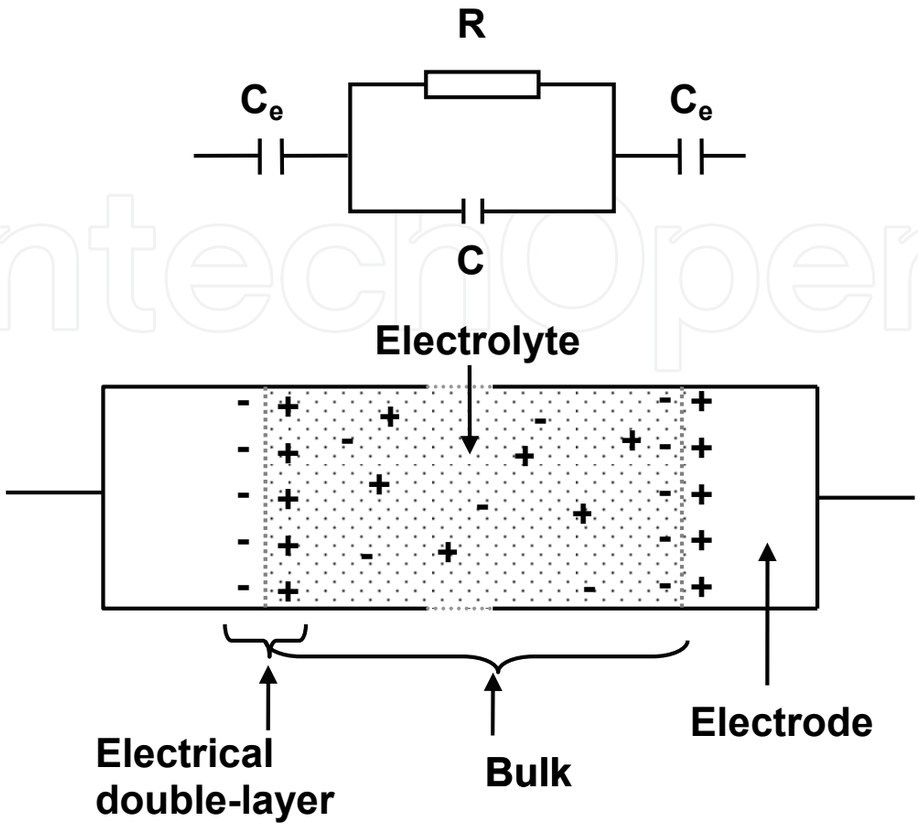

Fig. 1. Schematic diagram showing polarization in sample cell and simplified equivalent circuit for an electrolyte sandwiched between two blocking electrodes.

Using equations (6) and (7) the following equation can be obtained,

$$Z'' = -\left(\omega RCZ' + \frac{2}{\omega C_e} \right) \tag{8}$$

Actually, the Argand diagram of the complex impedance shows a semicircle with diameter R and a spike (straight line $Z'=R$) as seen in the schematic diagram in Figure 2 based on the assumption that C is very small compared to C_e since the thickness of the electrical double layer is of the order of the Debye length (λ), (that is, very small compared to the thickness of the electrolyte approximately 1 mm). The corresponding representation of equations (6) and (7) in the complex impedance plane is shown in Figure 3 and the real and the imaginary parts of the impedance versus frequency are shown in Figure 4 for a hypothetical case where R=1000 Ω, C=10 pF and C_e = 400 nF. The angular frequency corresponding to the maximum and the minimum of the imaginary part of the impedance is denoted by ω_1 and ω_2. Expressions for the frequencies corresponding to the maximum and minimum of Z'' can be derived under the assumption that C is very small compared to C_e. The angular frequency ω_1 corresponding to the maximum in Z'' shown in Fig. 3 can be obtained simply by substituting ($Z'=Z''=R/2$) in equations (6) or (7). Thus

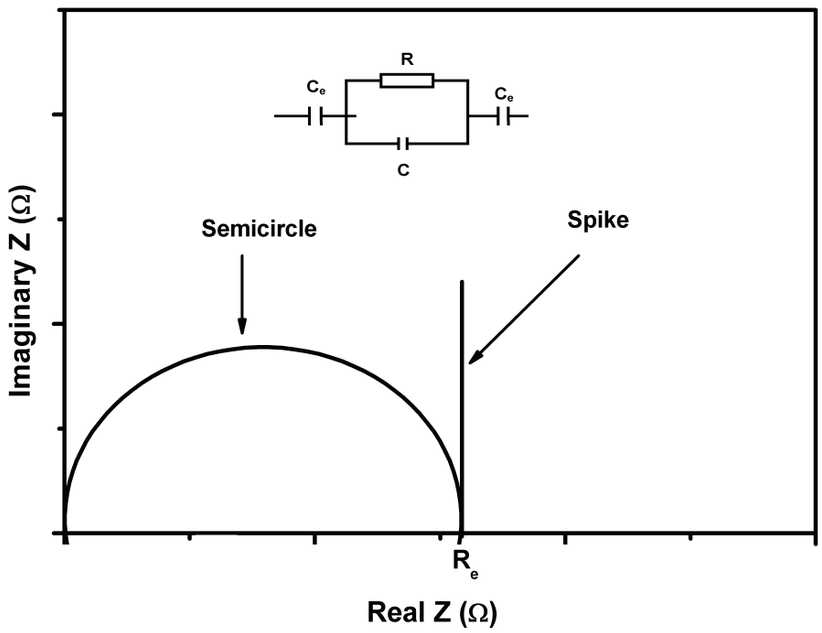

Fig. 2. Schematic diagram of equivalent circuit and the representation of real and imaginary parts of the impedance in a complex impedance plane based on the assumption that *C* is very small compared to C_e.

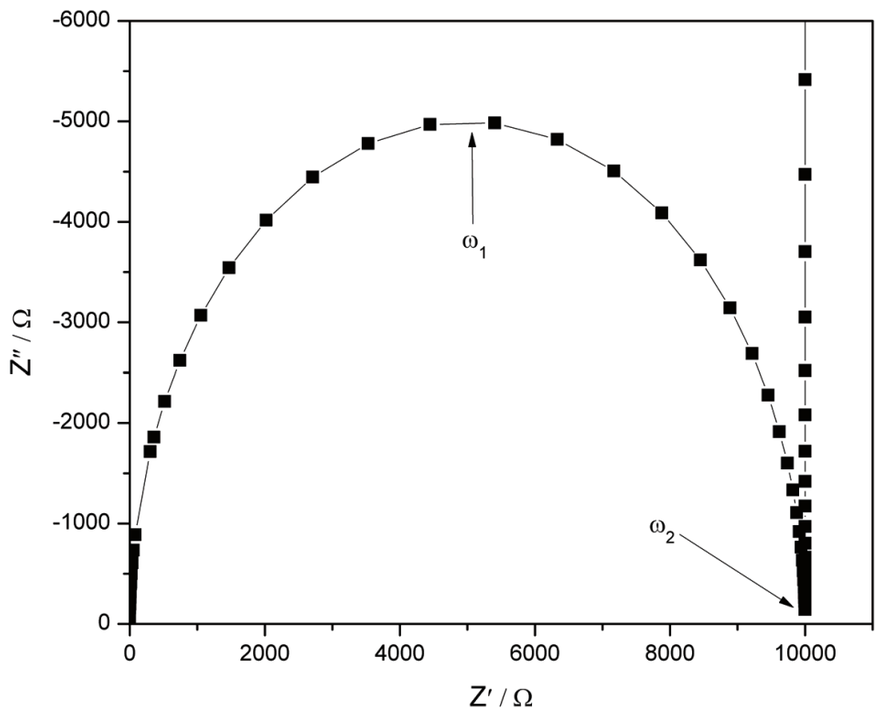

Fig. 3. The corresponding representation of equations (6) and (7) in the complex impedance plane for R=1000 Ω, C=10 pF and C_e = 400 nF.

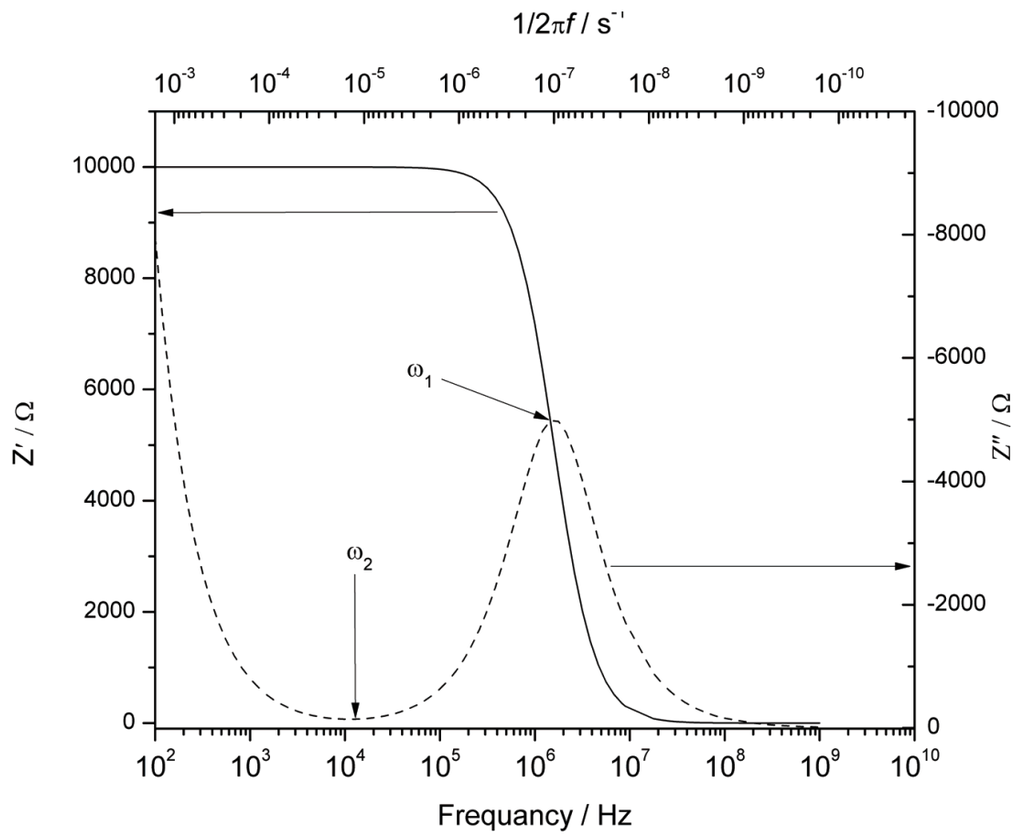

Fig. 4. The corresponding representation of equations (6) and (7), real and the imaginary parts of the impedance, as a function of frequency for R=1000 Ω, C=10 pF and C_e = 400 nF.

$$\omega_1 = \frac{1}{\tau_1} = \frac{1}{RC} \tag{9}$$

where τ_1 is characteristic time constant corresponding to the maximum in Z''. The angular frequency ω_2 corresponding to minimum in Z'' shown in Fig 3 can be obtained simply substituting ($Z'=R$, $Z''=0$) in equation (8). Then,

$$\omega_2 = \frac{1}{\tau_2} = \frac{1}{RC}\sqrt{\frac{2C}{C_e}} \tag{10}$$

where, τ_2 is the characteristic time constant corresponding to the minimum in Z''. For a cylindrical electrolyte sample of cross section area A, sample thickness $2d$ and mean thickness of the electrical double layer λ (equal to the Debye length) the R , C and C_e can be represented by;

$$R = \frac{2d}{\sigma_{dc} A} \tag{11}$$

$$C = \varepsilon_r \varepsilon_\circ \frac{A}{2d} \tag{12}$$

$$C_e = \varepsilon_r \varepsilon_\circ \frac{A}{\lambda} \tag{13}$$

where σ_{dc} is dc conductivity of the electrolyte, ε_r the dielectric constant of the electrolyte and $\varepsilon_\circ$ the vacuum permittivity. The R, C and C_e in equations (9) and (10) can be substituted using equations (11), (12) and (13) to obtain;

$$\omega_1 = \frac{1}{\tau_1} = \frac{\sigma_{dc}}{\varepsilon_\circ \varepsilon_r} = \frac{n\mu e}{\varepsilon_\circ \varepsilon_r} \tag{14}$$

$$\omega_2 = \frac{1}{\tau_2} = \frac{\sigma_{dc}}{\varepsilon_\circ \varepsilon_r \sqrt{\delta}} = \frac{n\mu e}{\varepsilon_\circ \varepsilon_r \sqrt{\delta}} \tag{15}$$

where $\delta = {}^{d}\!/_{\lambda} = {}^{C_e}\!/_{2C}$

Using equations (14) and (15) the relationship between τ_1 and τ_2 can be obtained,

$$\tau_2 = \tau_1 \sqrt{\delta} \tag{16}$$

According to Coelho [14], by modelling the macroscopic space-charge polarization, the effective permittivity $\tilde{\varepsilon}^*$ of an ionic conductor sandwiched between two blocking electrodes can be described by,

$$\tilde{\varepsilon}^* = \varepsilon_\circ \varepsilon_r \left\{ \left(\frac{1 + i\omega\tau_1}{i\omega\tau_1 + (\tanh Y)/Y} \right) \right\} \tag{17}$$

where Y is given by,

$$Y = (1 + i\omega\tau_1)^{1/2} \frac{d}{\lambda} \tag{18}$$

Using the approximation $\tanh(Y)/Y = (1 - i\omega\tau_1/2)/\delta$ valid for δ>>1, and recalling that δ is given by,

$$\delta = \frac{d}{\lambda} \tag{19}$$

equation (17) can be simplified to,

$$\tilde{\varepsilon}^* = \varepsilon'_\infty \left\{ \left(1 + \frac{\delta}{1 + (\omega\tau_1\delta)^2} \right) - i \left(\frac{\omega\tau_1\delta^2}{1 + (\omega\tau_1\delta)^2} \right) \right\} \tag{20}$$

where, $\varepsilon_\infty = \varepsilon'_\infty$ is high frequency permittivity,

The real (ε') and imaginary (ε'') parts of the dielectric constant as well as the dielectric loss tangent ($\tan\phi$) can be extracted from equation (20),

$$\varepsilon' = \varepsilon'_\infty \left(1 + \frac{\delta}{1 + (\omega\tau_1\delta)^2} \right) \tag{21}$$

$$\varepsilon'' = \varepsilon'_{\infty}\left(\frac{\omega\tau_1\delta^2}{1+(\omega\tau_1\delta)^2}\right) \tag{22}$$

$$\tan(\phi) = \frac{\varepsilon''}{\varepsilon'} = \frac{\omega\tau_1\delta^2}{1+\delta+(\omega\tau\delta)^2} \approx \frac{\omega\tau_1\delta}{1+\omega^2{\tau_1}^2\delta} \tag{23}$$

As illustrated in Appendix 1 it can be proved that the relaxation time τ_2 corresponds to the frequency of the maximum in dielectric loss tangent ($\tan\phi$). In this method the characteristic time constant τ_2 was chosen from the frequency at the maximum in $\tan(\phi)$. Hence, by using the relation $\tau_2 = \tau_1\sqrt{\delta}$ equation (20) can be modified to

$$\tilde{\varepsilon}^* = \varepsilon'_{\infty}\left\{\left(1+\frac{\delta}{1+(\omega\tau_2)^2\delta}\right) - i\left(\frac{\omega\tau_2\delta^{3/2}}{1+(\omega\tau_2)^2\delta}\right)\right\} \tag{24}$$

to take this characteristic time constant, τ_2, into account. It is noteworthy that the relaxation time τ_2 correspond to the frequency where the *dc* resistance is obtained from complex impedance plots and thus the real part of the impedance and the frequency dependence of the conductivity remains relatively unchanged close to this frequency, for an example, see Fig. 5 that shows the frequency dependence of the conductivity for KI solution electrolytes. Hence, graphical representations of the dielectric function can be used to extract τ_2. Fig. 6 shows the frequency dependence of the imaginary part of the dielectric constant (ε') and dielectric loss tangent ($\tan\phi$) if $\delta = 2\times10^4$ and $\tau_2 = 1.4\times10^{-7}$ s according to equation (24). On the other hand, when $\omega = 1/\tau_2$ the conductivity is in the *dc* limit and $\tau_2 >> \tau_1$. The net ionic diffusion coefficient (D) due to the conduction and diffusion in the electrolyte at the *dc* limit is given by;

$$\lambda = (D\tau_2)^{1/2} \tag{25}$$

For a single ion conductor, $D = D_{ion}$ can be used and in case both cations and anions are mobile, an effective D value may be used [17,18]. Anyhow, by using equation (18) one can obtain;

$$\delta = \frac{d}{(D\tau_2)^{1/2}} \tag{26}$$

Hence;

$$D = \frac{d^2}{\tau_2\delta^2} \tag{27}$$

As the diffusion coefficient, D, can be obtained using eqation (27), by means of dielectric data that gives τ_2 and δ, the well known Nernst-Einstein relation,

$$\mu = \frac{eD}{kT} \tag{28}$$

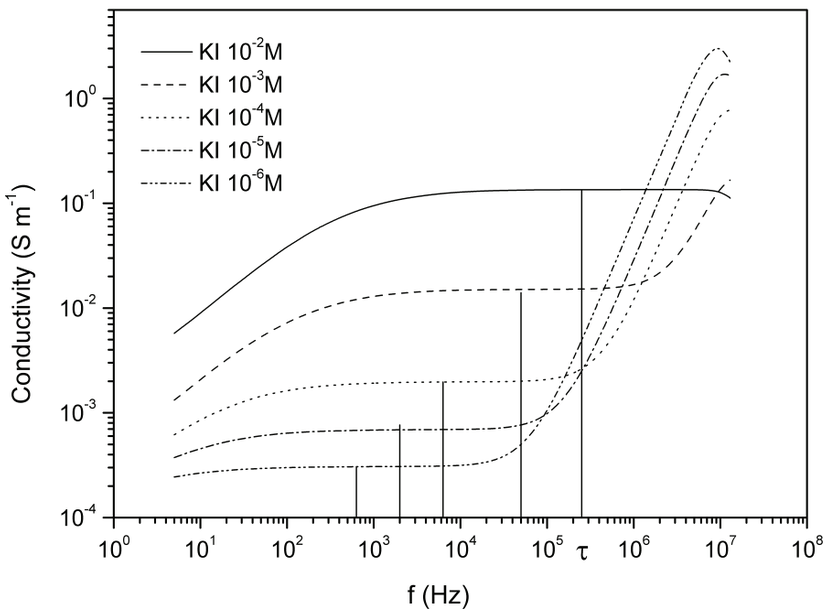

Fig. 5. The real part of the *ac* conductivity vs. frequency for 10^{-2}, 10^{-3}, 10^{-4}, 10^{-5}, 10^{-6} M KI solutions. The corresponding characteristic time constant, τ_2 , is also shown using a vertical line.

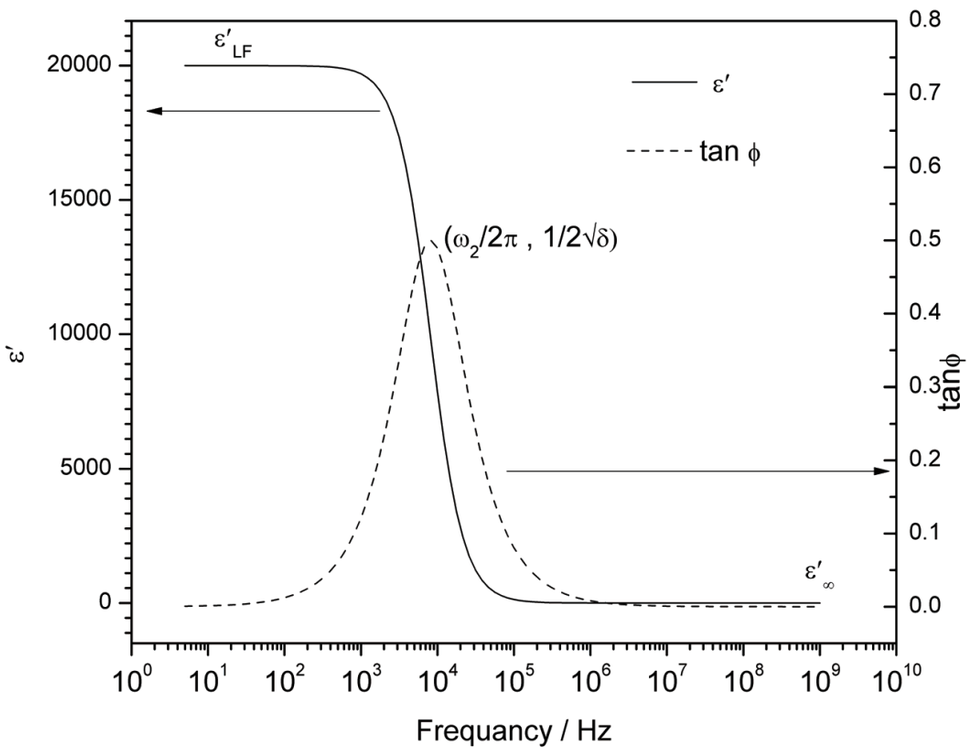

Fig. 6. The frequency dependent of imaginary part of the dielectric constant (ε´) and dielectric loss tangent ($\tan\phi = \varepsilon''/\varepsilon'$) according to equation (24) for $\delta = 2\times10^{4}$ and $\tau_2 = 1.4\times10^{-7}$ s.

where k is the Boltzmann constant and T the absolute temperature, can be used to deduce an equation for the mobility. Thus, μ can be obtained using equations (27) and (28).

$$\mu = \frac{ed^2}{kT\tau_2\delta^2} \tag{29}$$

In order to obtain the n value, μ in equation (4) is substituted into equation (29), thus

$$n = \frac{\sigma_{dc}kT\tau_2\delta^2}{e^2d^2} \tag{30}$$

If τ_2 and δ can be evaluated from dielectric measurement, equations (27) (29) and (30) can be used to determine D, μ and n values.

2.2 Determination of density and mobility of charge carriers

In order to calculate diffusion coefficient, mobility and mobile charge carrier density of an electrolyte values of τ_2 and δ should thus be obtained. There are actually many ways to estimate τ_2 and δ using electrical and dielectric measurements.

a. *Using Complex Impedance data*

Complex impedance data can be used to estimate τ_2 and δ. Using the frequencies corresponding to the maximum and minimum in Z'' values, ω_1 and ω_2 can be obtained, see Fig. 3. Hence, equations (14) – (16) can be used to calculate τ_2 and δ in order to determine diffusion coefficient, mobility and mobile charge carrier concentration.

b. *Using measured real part of the dielectric constant*

The frequency dependence of the measured real part of the dielectric constant can also be used to calculate τ_2 and δ. A schematic graph of the real part of the dielectric constant as a function of frequency is shown in Fig. 6. Curve fitting to the equation,

$$\varepsilon_r' = \varepsilon_\infty'\left(1 + \frac{\delta}{1+(\omega\tau_2)^2\delta}\right) \tag{31}$$

obtained using equation (24), can be used to estimate values for τ_2 and δ using measured data. In addition, as the Debye length is very small compared to sample thickness and thus the δ value is very large ($\delta >> 1$). Therefore, the low frequency limit in equation (31) can be used to derive an equation for δ,

$$\varepsilon_{LF}' = \varepsilon_\infty'(1+\delta) \tag{32}$$

Since $\delta >> 1$, δ is given by the equation

$$\delta = \frac{\varepsilon_{LF}'}{\varepsilon_\infty'} \tag{33}$$

Hence, the low and high frequency limits of the measured dielectric constant can be used in order to calculate δ using equation (33) see Fig 6. Equations (29) and (30) can also be modified to use the low and high frequency limits of ε'.

$$\mu = \frac{ed^2}{kT\tau_2}\left(\frac{\varepsilon'_\infty}{\varepsilon'_{LF}}\right)^2 \tag{34}$$

$$n = \frac{kT\sigma\tau_2}{e^2 d^2}\left(\frac{\varepsilon'_{LF}}{\varepsilon'_\infty}\right)^2 \tag{35}$$

c. *Using measured real part of the dielectric loss tangent*

According to this model, an equation for the dielectric loss tangent, $\tan\phi$, can be obtained using equation (24);

$$\tan\phi = \left(\frac{\omega\tau_2\sqrt{\delta}}{1+(\omega\tau_2)^2}\right) \tag{36}$$

Fig. 6 shows a typical example for dielectric loss tangent, $\tan\phi$, curve according to equation (36). The measured data for dielectric loss tangent can be fitted to equation (36) in order to estimate values for δ and τ_2. In addition, to estimate δ and τ_2 the coordinates at the peak value (maximum) in $\tan\phi$ can also be used (see Fig 6). The τ_2 can be calculated using the frequency corresponding to the maximum in $\tan\phi$ and δ can be estimated using the peak value of $\tan\phi$ as described in Appendix 1.

2.3 Real systems with blocking electrodes

The equations described above are valid for Debye type relaxations. In general, real systems do not follow exactly the behaviour described by these equivalent circuits and model equations. For example, the spike shown in Fig 2 is inclined and deformed due to electrode effects etc. Thus to broaden the applicability of the method to Cole-Cole type relaxations [19] the real and imaginary parts of the dielectric constant and dielectric loss tangent shown in equation can be modified to,

$$\varepsilon' = \varepsilon'_\infty\left(1+\frac{\delta}{1+(\omega\tau_m)^{2(1-\alpha)}\delta}\right) \tag{37}$$

$$\varepsilon'' = \varepsilon'_\infty\left(\frac{\omega\tau_2\delta^{3/2}}{1+(\omega\tau_2)^{2(1-\alpha)}\delta}\right) \tag{38}$$

$$\tan\phi = \left(\frac{\omega\tau_2\sqrt{\delta}}{1+(\omega\tau_2)^{2(1-\alpha)}}\right) \tag{39}$$

where, α is a constant ($\alpha < 1$) [19]. Dielectric measurements of real electrolyte systems with blocking electrodes can successfully be fit to equations (37) or (38) or (39) and values of δ and τ_2 can be estimated in order to calculate diffusion coefficient, charge carrier density and mobility.

3. Diffusion coefficient (*D*), charge carrier density (*n*) and mobility (*μ*)

3.1 *D, n* and *μ* in KI Solutions.

To test the applicability of the model 10^{-2} M KI and10^{-3} M KI solutions were investigated, the graphs of ε' vs. frequency are shown in Fig. 7. For KI solutions with lower concentrations (less than 10^{-4} M KI) the low frequency plateau appears outside the measured frequency window. The KI solutions with concentrations 10^{-2} M and 10^{-3} M KI showed more or less sigmoidal curves within the measured frequency range. The curves in Fig. 7 were fitted to equation (37) and the obtained parameters were used for the calculations. An appropriate ε'_{∞} value was determined using the plots in Fig. 7 prior to the curve fitting. During the fitting an appropriate α value was also selected. The α value was in the range 0.15 to 0.25 for both KI solutions. The fitted curves are also shown in Fig. 7 and the obtained parameters τ_2 and δ are given in Table 1. The low frequency plateaus of the experimental curves have an incline probably due to contributions from other low frequency relaxations apart from the space charge relaxation possibly due to electrode effects. To take such other relaxations into account the model will require modifications but the major concern of this chapter is the determination of the charge carrier density and the mobility in electrolytes by modelling the space charge relaxation. The selection of the appropriate frequency region for curve fitting (dominated by the space change relaxation) can improve the accuracy of the results. Accordingly, the low frequency region in Fig. 7 was omitted from fitting in order to reduce the errors due to other relaxation effects.

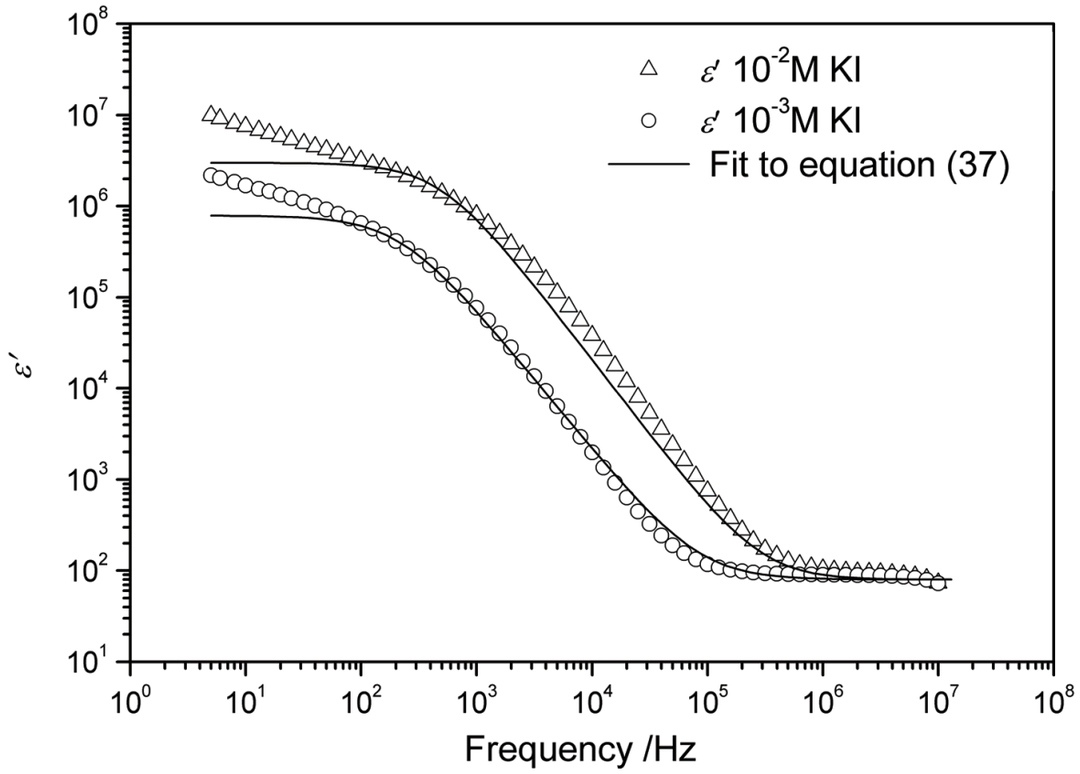

Fig. 7. The ε' versus frequency for 10^{-2} M and 10^{-3} M KI solutions at temperatures 25 °C. The solid lines represent curves fitted to equation (37).

The parameters τ_2 and δ extracted from curve fitting were used in equations (27), (29) and (30) to determine the D, n, and μ values shown in Table 1. The standard deviation of τ_2 and δ values obtained from the curve fitting remained less than 10% and the error in σ and T was maintained less than 5%. Based on this, the error limit of the n and μ values obtained in this method is estimated to be within ±20%.

KI Concentration	σ_{dc} /mS cm^{-1}	τ_2 /s	δ	D /m^2 s^{-1}	n /m^{-3}	μ /m^{2}V^{-1}s^{-1}
10^{-2} M	1.34	5.09×10^{-7}	46341.33	2.0×10^{-9}	1.09×10^{25}	7.7×10^{-8}
10^{-3} M	0.15	27.0×10^{-7}	9014.65	2.2×10^{-9}	1.11×10^{24}	8.6×10^{-8}

Table 1. The conductivity (σ_{dc}), fitting parameters (τ_2, δ), diffusion coefficient (D), charge carrier density (n) and mobility (μ) determined for 10^{-2} M and 10^{-3} M KI solutions at 25 °C.

Fig. 8 shows the dielectric loss tangent, $\tan\phi$, as a function of frequency for KI solutions with concentrations 10^{-2}, 10^{-3}, 10^{-4}, 10^{-5},10^{-6} M. In order estimate τ_2 and δ, $\tan\phi$ plots can also be used. For instance, curve fitting to equation (39) or the coordinates (τ_2, $\frac{\sqrt{\delta}}{2}$) of the maximum in $\tan\phi$ can be used to determine τ_2 and δ and then equations (29) and (30) can be used to calculate the mobility and charge carrier density.

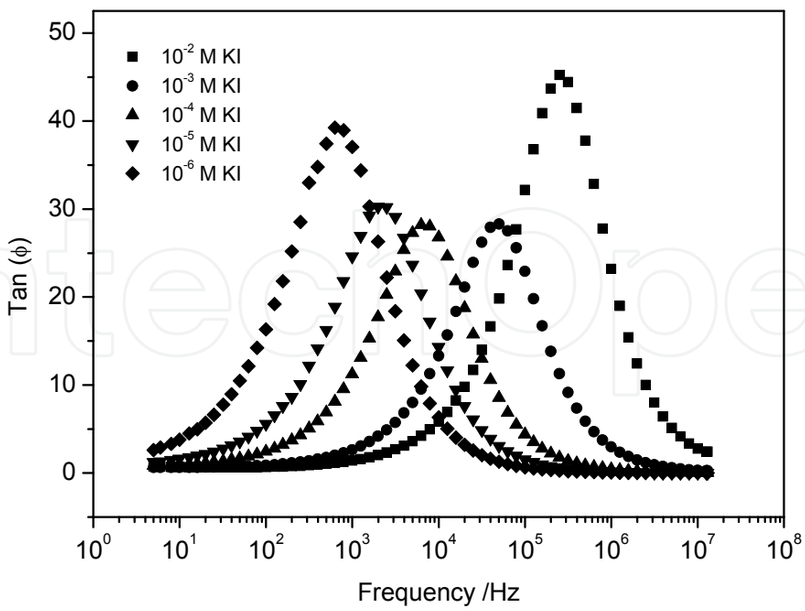

Fig. 8. Dielectric loss tangent, $\tan\phi$ vs. frequency for 10^{-2}, 10^{-3}, 10^{-4}, 10^{-5}, 10^{-6} M KI solutions at 25 °C.

3.2 *D*, *n* and *μ* in the Ionic Liquid, 1-methyl-3 propyl imidazolium iodide

This method of calculating mobility and charge carrier density was applied to estimate the n, μ and D values for the ionic liquid 1-methyl-3 propyl imidazolium iodide which is a useful electrolyte material for solar cell applications. Some of the fitted curves and measured data are shown in Figure 9 in the temperature range 8 to 60 °C. The reliability of the model equations for this ionic liquid was established by the excellent fitting of the measured data to equation (37) as shown in Figure 9. In fact, the data fitted well and the standard deviations of δ and τ values were less than 2 %. The values of n, μ and D calculated using this method are shown in Fig. 10 and 11. The conductivity values obtained directly from impedance measurements are also shown in Fig. 10. It can be immediately seen that in this system, the increase in conductivity with increasing temperature is dominated by the increase in the charge carrier concentration rather than by the increase in the mobility.

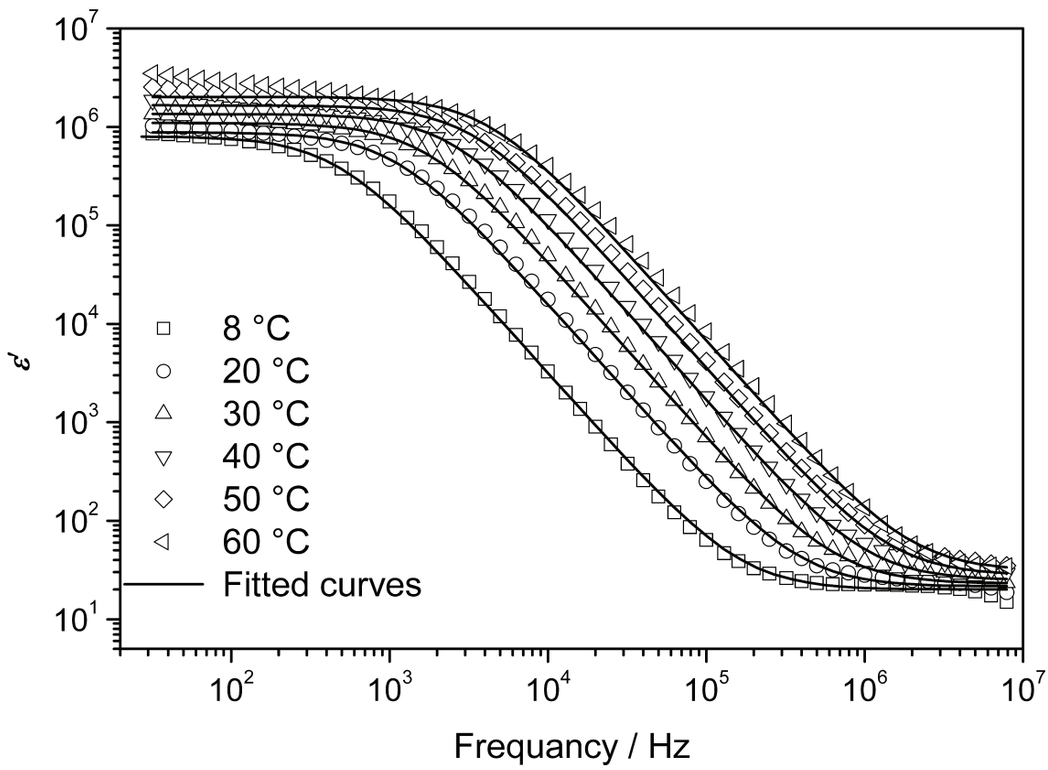

Fig. 9. The measured real part of the dielectric constant (ε') and the fitted curves to model equation (37) for ionic liquid, 1-methyl-3-propyl imidazolium iodide, at different temperatures.

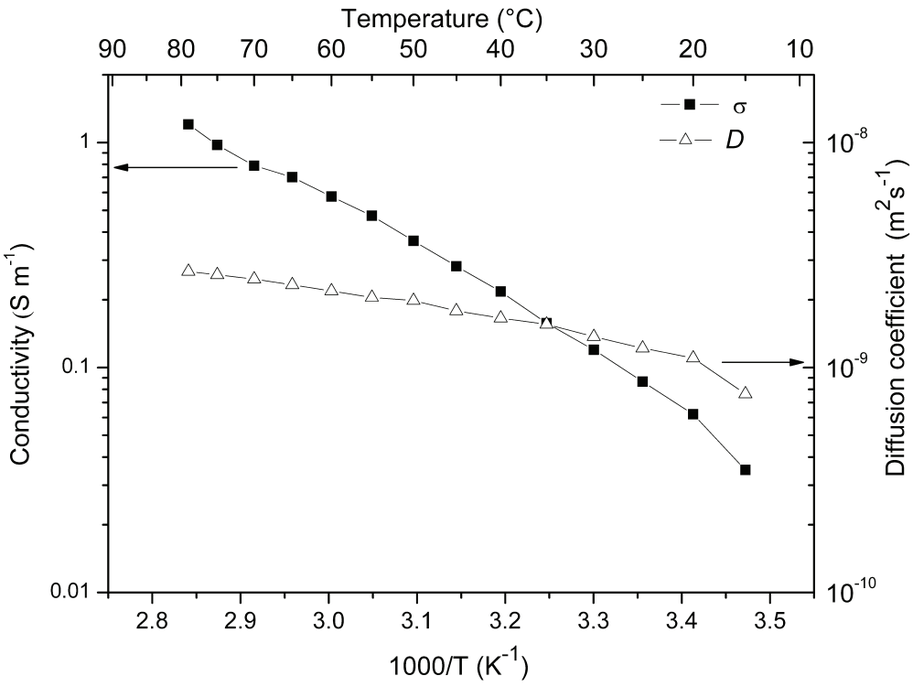

Fig. 10. The conductivity, σ, and diffusion coefficient, *D*, versus 1000/*T* for the ionic liquid, 1-methyl-3-propyl imidazolium iodide.

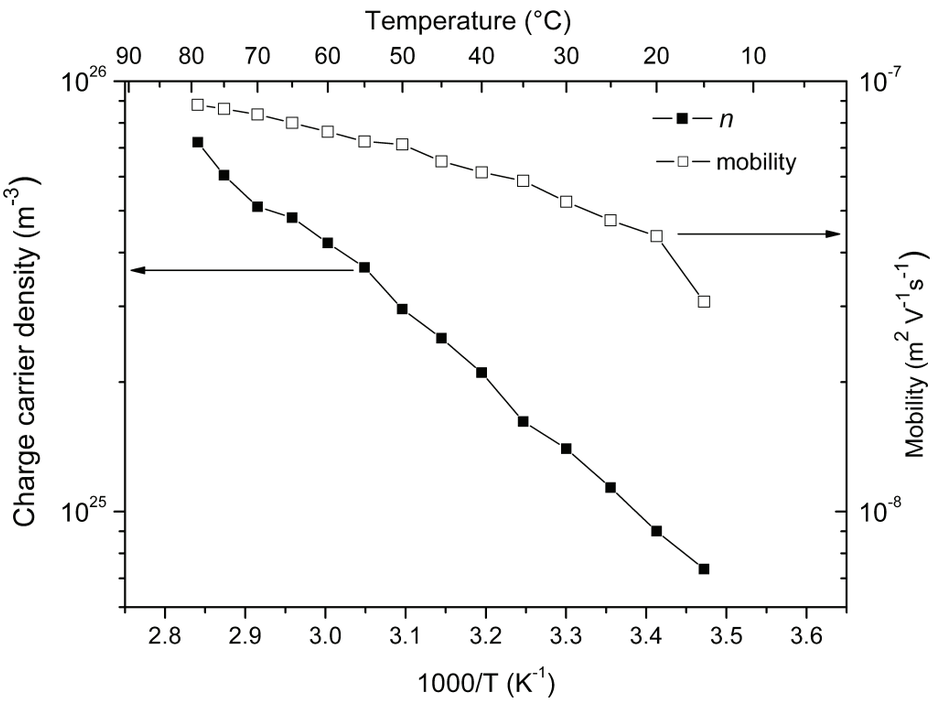

Fig. 11. The charge carrier density, *n*, and the mobility, *μ*, calculated using the new method, as a function of 1000/T for the ionic liquid, 1-methyl-3-propyl imidazolium iodide, at different temperatures.

Fig. 11 shows the dielectric loss tangent, $\tan\phi$, as a function of frequency for 1-methyl-3-propyl imidazolium iodide, at different temperatures. In order to estimate τ_2 and δ this $\tan\phi$ plots can also be employed.

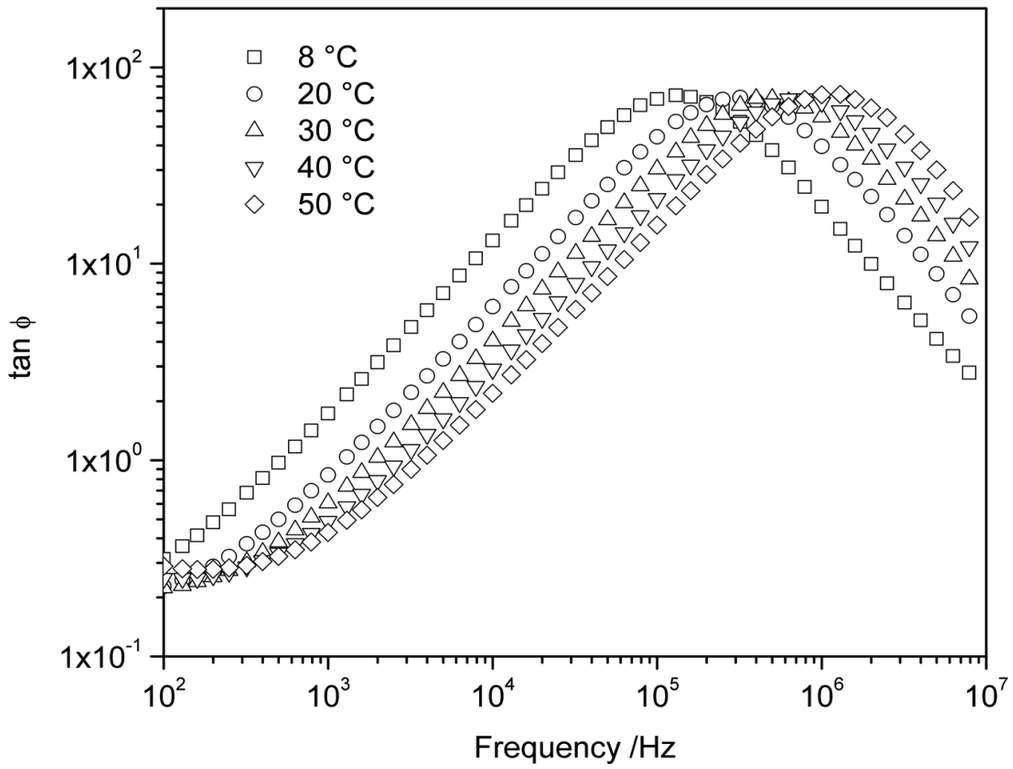

Fig. 12. The measured dielectric loss tangent as a function of frequency for the ionic liquid, 1-methyl-3-propyl imidazolium iodide, at different temperatures.

3.3 *D*, *n* and *μ* in 1-Butyl-1-methylpyrrollidinum bis(tryfluoromethanesulfonyl) imide

The method was employed to estimate the n, μ and D values in the ionic liquid 1-Butyl-1-methylpyrrolidinum bis(trifluoromethanesulfonyl) imide ($PYR_{14}TSFI$). Some of the fitted curves and measured data in the temperature range 0 to 50 °C for this ionic liquid are shown in Figure 13. The measured data for this ionic liquid also showed a good fit to equation (37) as shown in Figure 13, demonstrating the applicability of the method to this ionic liquid. The values obtained for the standard deviation of δ and τ was less than 5 %. The values of n, μ and D calculated using this method are shown in Fig. 14 and 15. The conductivity values obtained directly from impedance measurements are also shown in Fig. 14 for $PYR_{14}TSFI$. It can be inferred that the increase in conductivity with increasing temperature is dominated by the increase in the mobility rather than by the increase in the charge carrier concentration in this system.

Fig. 16 shows the dielectric loss tangent, $\tan\phi$, as a function of frequency for $PYR_{14}TSFI$, at different temperatures. In order to estimate τ_2 and δ these $\tan\phi$ plots can also be used. Curve fitting to equation (39) or coordinates of the maximum in $\tan\phi$ can be used to determine τ_2 and δ.

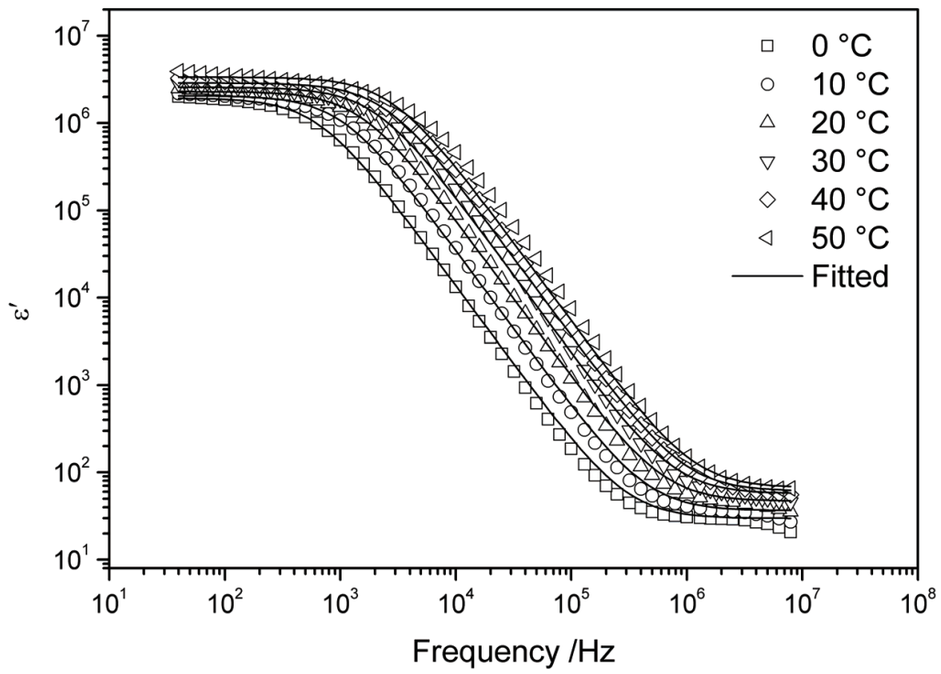

Fig. 13. The measured real part of the dielectric constant (ε') and the fitted curves to model equation (37) for the ionic liquid, $PYR_{14}TSFI$, at different temperatures.

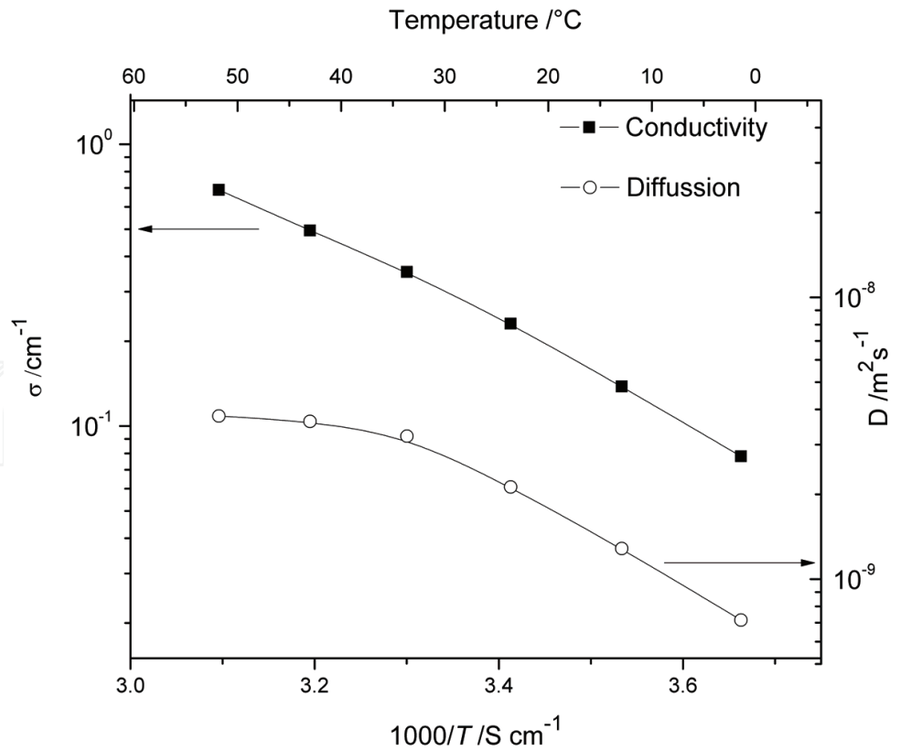

Fig. 14. The conductivity, σ, and diffusion coefficient, D, obtained using impedance measurements, versus $1000/T$ for the ionic liquid, $PYR_{14}TSFI$.

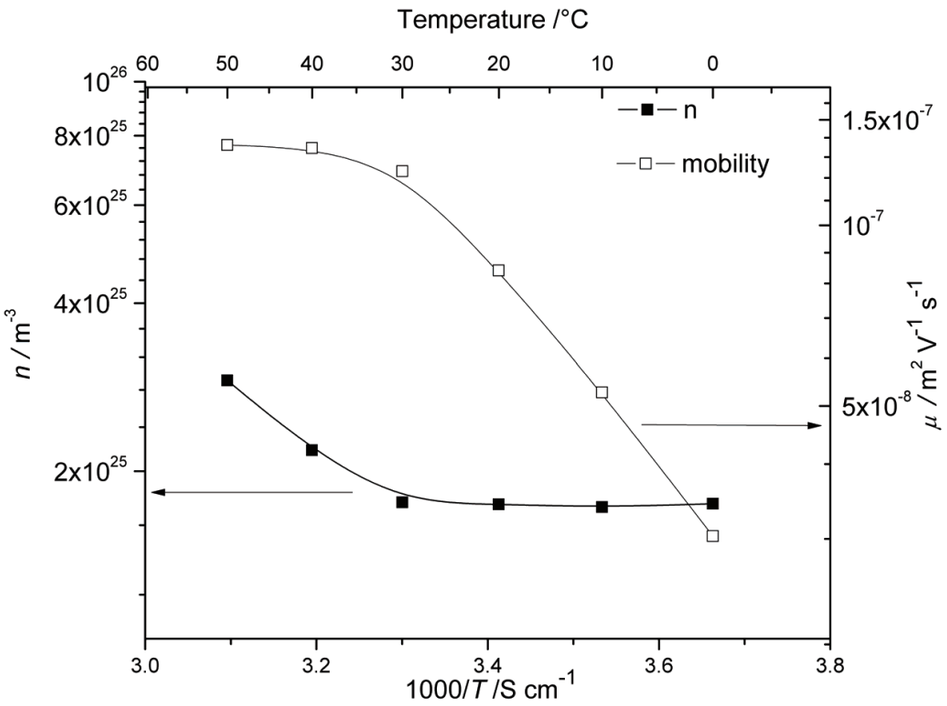

Fig. 15. The charge carrier density, n, and the mobility, μ, calculated using the new method, as a function of 1000/T for the ionic liquid, $PYR_{14}TSFI$, at different temperatures.

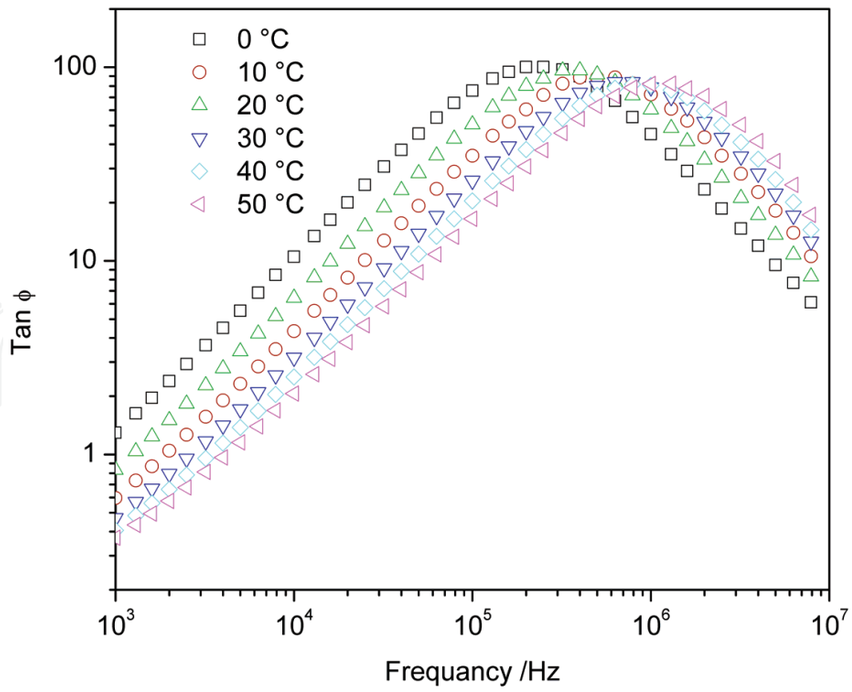

Fig. 16. The measured the dielectric loss tangent as a function of frequency for ionic liquid, $PYR_{14}TSFI$, at different temperatures.

3.4 *D*, *n* and *μ* in a polymer electrolyte containing an ionic liquid.

An iodide ion (I^-) conducting polymer electrolyte, based on polyethylene oxide (PEO) and tetrahexylammonium iodide ($Hex_4N^+I^-$) salt was selected for application of the method [20]. The electrolyte contained ethylene carbonate (EC) 100% mass fraction and $Hex_4N^+I^-$ 60% mass fraction with respect to the weight of PEO in the electrolyte. The measured real part of the dielectric constant and the fitted curves for the PEO/$Hex_4N^+I^-$/EC electrolyte for different temperatures are shown in Fig 17. The obtained conductivities from impedance measurements for the PEO/$Hex_4N^+I^-$/EC electrolyte samples are shown in Fig. 18 and the diffusion coefficient, *D*, calculated using curve fitted parameters is also shown in Fig. 18. The charge carrier density, *n,* and the mobility μ calculated using this method are shown in Fig 19. The model equation (37) fitted rather well giving less than 5% standard deviation, thus exhibiting the reliability of the model equations. This type of electrolytes show two melting peaks that relates to the PEO rich phase and the EC rich phase at about 60 °C and 30 °C [20]. Before melting theses phases in the PEO/$Hex_4N^+I^-$/EC electrolyte shows high mobility values and low charge carrier density. In general, for temperatures higher than 30 °C both the mobility and density of charge carriers increases with increasing temperature.

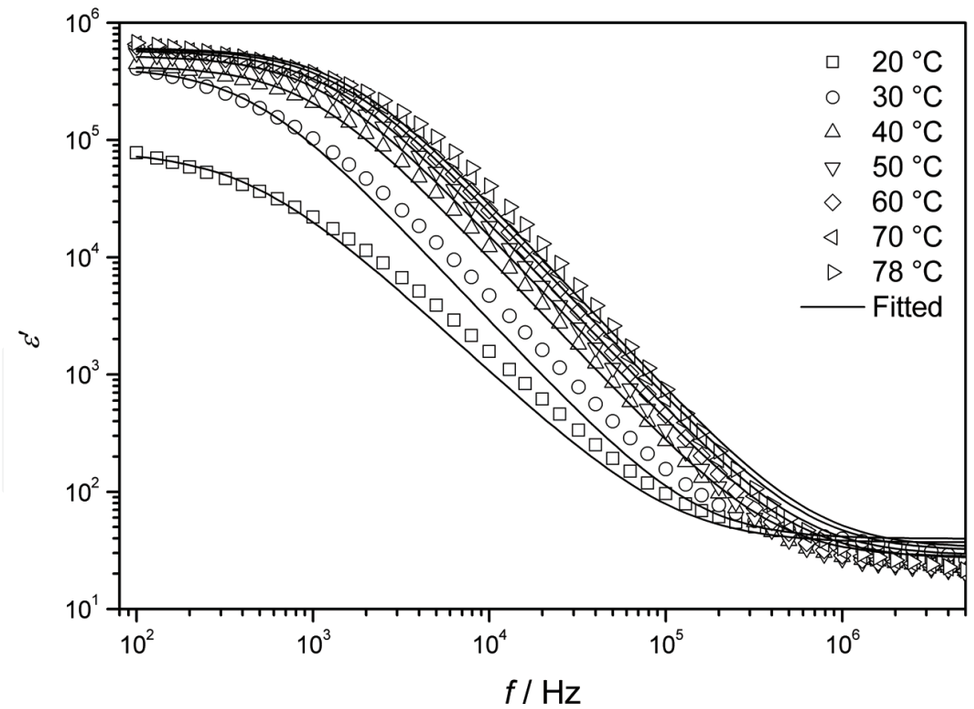

Fig. 17. The measured real part of the dielectric constant (ε') and the fitted curves to model equation (37) for PEO/$Hex_4N^+I^-$/EC electrolyte at different temperatures

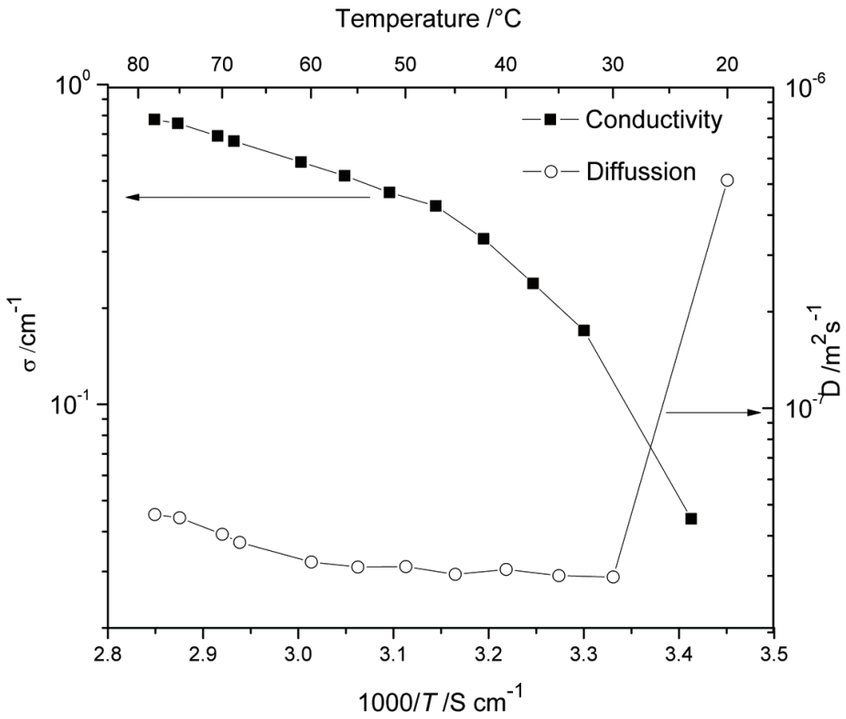

Fig. 18. The conductivity, obtained using impedance measurements, versus 1000/T for PEO/$Hex_4N^+I^-$/EC electrolyte.

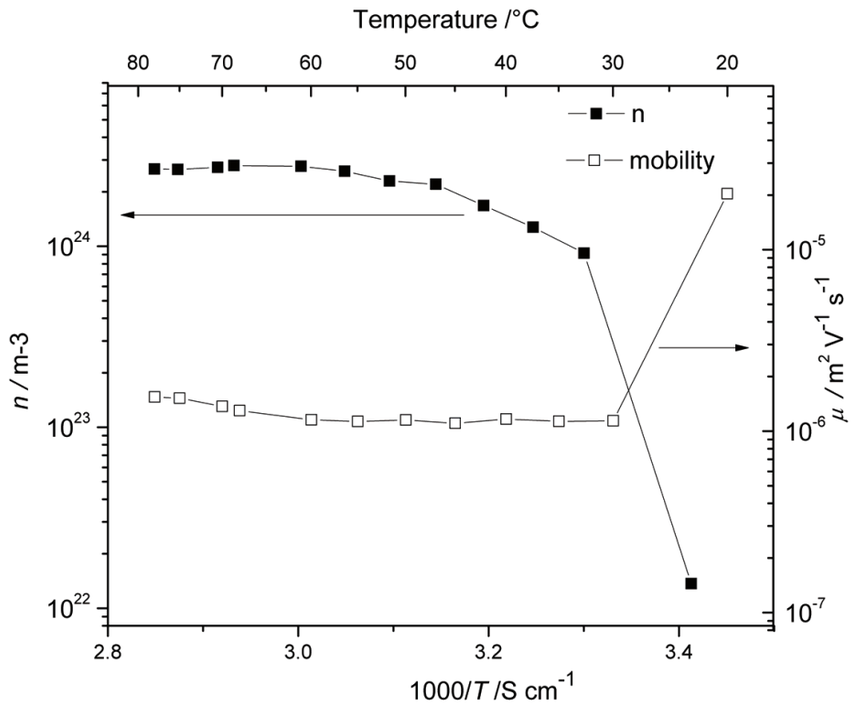

Fig. 19. The charge carrier density, n, and mobility, μ, calculated using the new method, as a function of 1000/T for PEO/$Hex_4N^+I^-$/EC.

3.5 The n and μ in a KI solution without curve fitting

The complex impedance measurements are the basis for the evaluation of μ and n and the complex impedance measurements can actually be directly employed to determine τ_2 and δ. As another test measurements on aqueous solutions were made using KI. Figure 20 shows the graph of imaginary part of the complex impedance Z'' against the real part Z' for 3×10^{-4} M solution at different temperatures. The relaxation time, τ_2, was obtained from the frequency corresponding to the minimum in Z'' shown in Figure 20. This τ_2 value coincides with the frequency of the maximum in $\tan\phi$ as described in the theory section.

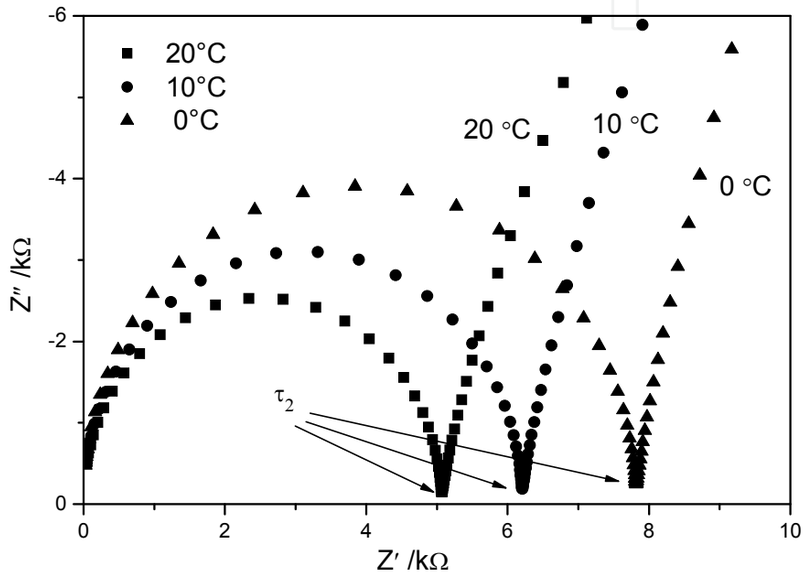

Fig. 20. Complex part of the impedance (Z'') versus real part of the impedance (Z') for the 3×10^{-4} M KI solution at 0, 10 and 20 °C respectively.

The graphs given in Fig. 21 show the real part of *ac* conductivity as a function of frequency for 10^{-2} M and 10^{-3} M KI concentration at temperatures between 0 and 20 °C. The curves have the expected appearance and σ can be extracted from either the value of Z' at the minimum Z'' in Fig. 20 or from the plateau values of the graphs in Fig. 21.

The ε' vs frequency curves have the expected appearance, however, for lower concentrations (10^{-4} M KI) the ε'_{LF} is difficult to estimate as it is shifting outside the measurement window. 10^{-3} M and10^{-2} M KI solutions gave relatively sigmoidal curves within the measurement window.

The σ_{dc} , τ_2 and δ ($\varepsilon'_{LF}/\varepsilon'_{\infty}$) values were determined using the plots shown in Figures 20, 21 and 22. However, the determination of ε'_{LF} was difficult due to the inclination of the low frequency plateau of ε' , which, in turn, is due to the existence of other relaxations apart from the space charge relaxation. In order to improve accuracy, a method to properly determine ε'_{LF} is needed when curve fitting is not used. The n and μ values were in this case determined using equations (34) and (35) and the calculated values are shown in Tables 2 and 3. The obtained values differ somewhat compared to those obtained using curve fitting.

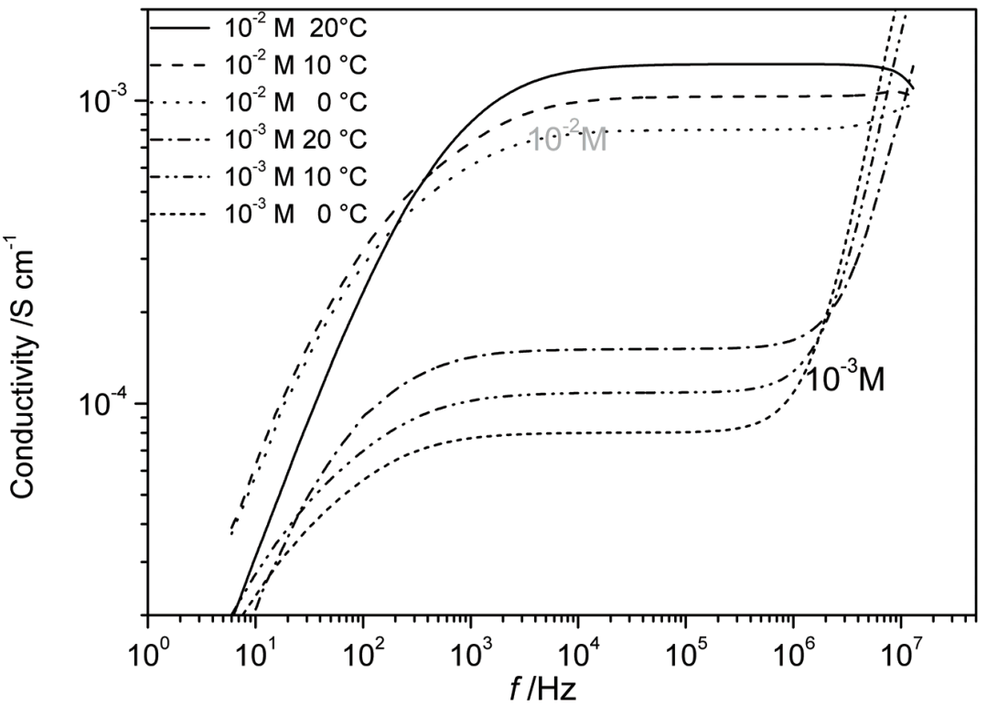

Fig. 21. Conductivity isotherms for 10^{-2} M and 10^{-3} M KI solutions as a function of frequency for temperatures 0, 10 and 20 °C.

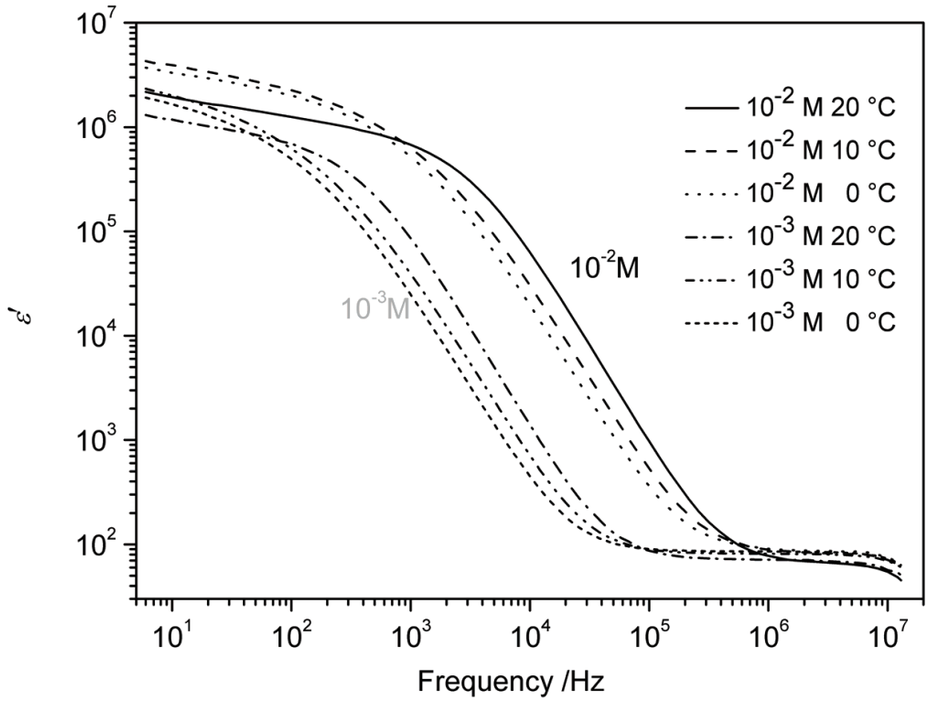

Fig. 22. The ε' versus frequency for 10^{-2} M and 10^{-3} M KI solutions at temperatures 0, 10 and 20 °C.

The evaluation done without curve fitting is generally regarded as less reliable as long as the determination of ε'_{LF} is uncertain. However, this method is simple and convenient in cases were reliable data are available.

Temperature (°C)	σ (mS m^{-1})	$\tau_m \times 10^{-6}$ (s)	$\varepsilon'_{LF}/\ \varepsilon'_\infty \times 10^4$	$D \times 10^{-9}$ (m^2 s^{-1})	$n \times 10^{24}$ (m^{-3})	n%	$\mu \times 10^{-7}$ (m^{2}V^{-1}s^{-1})
20	1.3	4.154	1.291	1.36	1.52	127	5.42
10	1.1	6.097	1.152	1.16	1.42	118	4.44
0	0.8	7.387	1.101	1.05	1.12	93	4.38

Table 2. Calculated n, and μ values for 10^{-3} M KI, with parameters σ_{dc} , τ_2 and δ (=$\varepsilon'_{LF}/\varepsilon'_\infty$)

Temperature (°C)	σ (mS m$^{-1)}$	$\tau_m \times 10^{-7}$ (s)	$\varepsilon'_{LF}/\ \varepsilon'_\infty \times 10^4$	$D \times 10^{-9}$ (m^2 s^{-1})	$n \times 10^{25}$ (m^{-3})	n%	$\mu \times 10^{-8}$ (m^{2}V^{-1}s^{-1})
20	12	5.03	4.995	1.34	1.4	117	5.3
10	10	7.38	4.778	1.40	1.3	114	4.7
0	08	10.76	3.988	0.98	1.2	100	4.2

Table 3. Calculated values for 10^{-2} M KI the values are shown in the order they were performed

4. Conclusions

Finally, it can be concluded that the mobile charge carrier density of electrolytes can be obtained from the expression $\frac{\sigma kT\tau_m\delta^2}{e^2d^2}$ and mobility can be obtained from $\frac{ed^2}{kT\tau_m\delta^2}$. It is applicable for aqueous electrolytes, ionic liquids and plasticized polymer electrolyte containing ionic liquids. Use of curve fitting is a reliable and convenient method for the proper estimation of the parameters. However the mobility and density of mobile ions can be calculated even without using curve fitting.

Appendix 1

At frequencies close to the maximum in $\tan\phi$ both the Z'' and ε'' values are close to minimum and the electric displacement remains constant. Furthermore, the conductivity is in its *dc* limit and effects of ionic and dipole polarizations are negligible since they take place at lower frequencies.

τ_m is the relaxation time corresponding to the frequency where $\tan\phi$ shows a maximum. According to equation (23) the dielectric loss tangent is given by;

$$\tan(\phi) = \frac{\varepsilon''}{\varepsilon'} = \frac{\omega\tau\delta^2}{1+\delta+(\omega\tau\delta)^2} \approx \frac{\omega\tau\delta}{1+\omega^2\tau^2\delta} \tag{40}$$

When $\tan\phi$ is maximum

$$\frac{d}{d\omega}\tan(\phi) = 0 = \frac{\tau\delta((1+\omega^2\tau^2\delta) - 2\omega^2\tau^3\delta^2}{(1+\omega^2\tau^2\delta)} \tag{41}$$

$$\text{thus } \omega_m{}^2\tau^2\delta = 1 \tag{42}$$

$$\text{Therefore } \tau_m = \tau\sqrt{\delta} = \tau_2 \tag{43}$$

$$\text{thus } \tan(\phi)_{Max} = \frac{\sqrt{\delta}}{2} \tag{44}$$

5. References

[1] A. Radu, A.J. Meir, E. Bakker, Anal. Chem.,74 (2004) 6402-6409.
[2] S. Sodaye, G. Suresh, A.K. Pandy, A. Goswami, J. Membrane Science, 295 (2007) 108-113.
[3] Y.M. Scindia, A.K. Pandey, A.V.R. Reddy, S.B. Manohar, Anal. Chem., 74 (2004) 4204-4212.
[4] F. M. Gray, Solid Polymer electrolytes fundamentals and technological applications Vol. (1991)VCH Publishers, New York, 1-4.
[5] A.K. Shukla, A.S. Arico, V. Antonucci, Renewable and Sustainable Energy Reviews 5 (2001) 137–155.
[6] M. Jönsson, K. Welch, S. Hamp, M Stromme, J. Phys. Chem. B, 110 (2006) 10165 -10169.
[7] M. Watanabe, S. Nagano, K. Sanui, and N. Ogata, Solid State Ionics, 911 (1988) 28.
[8] M. Watanabe, S. Nagano, K. Sanui, and N. Ogata, Solid State Ionics, 338 (1986) 18–19.
[9] K. Hayamizu, E. Akiba, T. Bando, Y. Aihara, J. Chem. Phys. (2002) 117-12, 5929-5939
[10] R.C. Agrawal, R. Kumar. R. K. Gupta, Materials Science and Engineering B57 (1998) 46-51.
[11] R.J. Klein, S. Zhang, S. Dou, B. H. Jones,R. H. Colby, J. Runt, J. Chemical Physics 124, (2006) 144903-8.
[12] Niklasson, G. A.; Jonsson, A. K.; Stromme, M. Impedance Response of Electrochromic Materials and Devices. In *Impedance Spectroscopy*, 2nd ed.; Barsoukov, Y., Macdonald, J. R., Eds.; Wiley: New York, 2005 (302-326).
[13] H.J Schütt, Solid State Ionics, 505 (1994) 70-71.
[14] R. Coelho, Physics of Dielectrics, Elsevier Scientific Publishing Company, New York 1979 pp 97-102.
[15] H.J. Schütt and E. Gerdes, Journal of Non-Crystalline Solids, 144 (1992) 1-13.
[16] H.J. Schütt and E. Gerdes, Journal of Non-Crystalline Solids, 144 (1992) 14-20.
[17] S. Bhattacharja, S. W. Smoot, D. H. Whitmore, Solid State Ionics, 18-19, (1986) 306-314.
[18] P.G. Bruce, C. A. Vincent, Faraday Discuss. Chem. Soc., 88, (1989) 43-54.
[19] K.S. Cole, R.H. Cole, J. Chem. Phys. 9 (1941) 341-51.
[20] T. M. W. J. Bandara, P. Ekanayake, M. A. K. L. Dissanayake, I. Albinsson, B.-E. Mellander, J. Solid State Electrochem. DOI 10.1007/s10008-009-0951-x

Ionic Liquids: Theory, Properties, New Approaches
Edited by Prof. Alexander Kokorin

ISBN 978-953-307-349-1
Hard cover, 738 pages
Publisher InTech
Published online 28, February, 2011
Published in print edition February, 2011

Ionic Liquids (ILs) are one of the most interesting and rapidly developing areas of modern physical chemistry, technologies and engineering. This book, consisting of 29 chapters gathered in 4 sections, reviews in detail and compiles information about some important physical-chemical properties of ILs and new practical approaches. This is the first book of a series of forthcoming publications on this field by this publisher. The first volume covers some aspects of synthesis, isolation, production, modification, the analysis methods and modeling to reveal the structures and properties of some room temperature ILs, as well as their new possible applications. The book will be of help to chemists, physicists, biologists, technologists and other experts in a variety of disciplines, both academic and industrial, as well as to students and PhD students. It may help to promote the progress in ILs development also.

INTECH
open science | open minds

InTech Europe
University Campus STeP Ri
Slavka Krautzeka 83/A
51000 Rijeka, Croatia
Phone: +385 (51) 770 447
Fax: +385 (51) 686 166
www.intechopen.com

InTech China
Unit 405, Office Block, Hotel Equatorial Shanghai
No.65, Yan An Road (West), Shanghai, 200040, China
中国上海市延安西路65号上海国际贵都大饭店办公楼405单元
Phone: +86-21-62489820
Fax: +86-21-62489821

IntechOpen